Molecular Vibrations and Structures of High Polymers. V.[*1] *The Infrared Active Normal Vibrations of Isotactic Polypropylene, Poly(propylene-2-d), Poly(propylene-1, 1-d_2) and Poly(propylene-3, 3, 3-d_3) in the 1500 ~ 650 cm^{-1} Region*

By Tatsuo MIYAZAWA and Yoshiko IDEGUCHI

(Received May 25, 1963)

Isotactic polypropylene $[-CH_2-CH(CH_3)-]_n$ is structurally typical of a large number of isotactic polymers. Detailed infrared studies of isotactic polypropylene would provide the basic knowledge necessary for vibrational analyses and structure studies of other isotactic polymers. The infrared spectra of isotactic polypropylene and its deuterated derivatives have been measured, and empirical vibrational assignments have been made.[1-6] The effect of isotopic substitutions of the CH, CH_2, and CH_3 groups upon the infrared spectra have been found to be quite complicated. Except for the bands arising from the CH_3 symmetric or asymmetric deformation vibrations or for the bands due to the CH_2 bending vibrations, all the infrared bands in the 1500~650 cm^{-1} region have been found to shift more or less upon the deuterium substitution of any of the CH, CH_2, and CH_3 groups. Therefore, from empirical analyses of the observed isotope effects, all these bands have been considered to be due to hybridized modes of the CH, CH_2, and CH_3 groups.[4] Accordingly, the normal coordinate analyses are indispensable in elucidating the nature of the infrared bands observed for polypropylene and deuterated derivatives.

In our previous studies, general methods were worked out for treating normal vibrations of infinite helical polymers belonging to dihedral groups[7] (for example, polyethylene glycol) or those belonging to cyclic group[8] (for example, isotactic polypropylene). The infrared active normal vibrations of isotactic polypropylene were calculated[8] by the use of the modified Urey-Bradley potential function,[9,10] where the potential constants were transferred from aliphatic hydrocarbons.[11]

The polarized far-infrared spectra of isotactic polypropylene were measured in the 600~280 cm^{-1} region[8] and also in the 400~80 cm^{-1} region, and all the low-frequency infrared active normal vibrations were observed.[12] The normal vibrations of isotactic polypropylene were calculated by the use of the modified Urey-Bradley force field as supplemented by the internal rotation potential about the axial and equatorial C–C bonds and the C-methyl bonds,[13] and the nature of the low-frequency infrared bands were elucidated.[12]

*1 Presented at the Annual Meeting of the Chemical Society of Japan, Tokyo, March, 1963.

1) M. Peraldo and M. Farina, *Chim. e l'Inds.* (*Milano*), **42**, 1349 (1960).
2) C. Y. Liang and F. G. Pearson, *J. Mol. Spectr.*, **5**, 290 (1960).
3) C. Y. Liang, M. R. Lytton and C. J. Boone, *J. Polymer Sci.*, **47**, 139 (1960).
4) C. Y. Liang, M. R. Lytton and C. J. Boone, ibid., **54**, 523 (1961).
5) H. Tadokoro, T. Kitazawa, S. Nozakura and S. Murahashi, This Bulletin, **34**, 1209 (1961).
6) M. P. McDonald and I. M. Ward, *Polymer, Lond.*, **2**, 341 (1961).
7) T. Miyazawa, *J. Chem. Phys.*, **35**, 693 (1961).
8) T. Miyazawa, Y. Ideguchi and K. Fukushima, ibid., **38**, 2709 (1963); International Symposium on Molecular Structure and Spectroscopy, A120, Tokyo, September, 1962.
9) T. Shimanouchi, International Symposium on Molecular Structure and Spectroscopy, C216, Tokyo, September, 1962.
10) M. Tasumi, T. Shimanouchi and T. Miyazawa, *J. Mol. Spectr.*, **9**, 261 (1962).
11) H. Takahashi, *J. Chem. Soc. Japan, Pure Chem. Sec.* (*Nippon Kagaku Zasshi*), **83**, 976 978, 980 (1962).
12) T. Miyazawa, K. Fukushima and Y. Ideguchi, *Polymer Letters*, **1**, 385 (1963), 16th Annual Meeting of the Chemical Society of Japan, Tokyo, March, 1963.
13) T. Miyazawa and K. Fukushima, 16th Annual Meeting of the Chemical Society of Japan, Tokyo, April, 1963.

Unfortunately, however, the far-infrared spectra of the deuterated derivatives of isotactic polypropylene have not yet been published. In the present study, therefore, vibrational analyses were made of the infrared bands of isotactic polypropylene and deuterated derivatives observed in the 1500~650 cm^{-1} region.

Normal Coordinate Treatment

The normal vibrations of isotactic polypropylene, $[-CH_2-CH(CH_3)-]_n$; poly(propylene-2-d), $[-CH_2-CD(CH_3)-]_n$; poly(propylene-1,1-d_2), $[-CD_2-CH(CH_3)-]_n$; and poly(propylene-3,3,3-d_3), $[-CH_2-CH(CD_3)-]_n$ were treated in the present research. The high-frequency C–H stretching modes of the CH, CH_2, and CH_3 groups were separated in a manner described previously.[8] The internal rotation modes about the C–C bonds were not taken into account since the contributions of the internal rotation potential are not appreciable for the vibrations of polypropylene lying above 650 cm^{-1}. An NEAC model 2101 digital computer (Nippon Electric Company, Ltd., Tokyo) was used for the numerical computations involved in the normal coordinate treatment. The $\boldsymbol{G}$ and $\boldsymbol{F}$ matrices[14] for the degenerate normal vibrations of isotactic polypropylene were constructed and diagonalized according to a method described previously.[8]

The internal coordinate (or local symmetry coordinate) vectors, R_n, of the n-th repeating unit are,

where Δr's are the stretching coordinates for which the numbering of carbon and hydrogen atoms are shown in Fig. 1. The elements of the vector $\phi(CH)_n$ in Eq. 1, are; $\Delta\phi(2,n-1;1,n;3,n)$, $\Delta\phi(2,n-1;1,n;5,n)$, $\Delta\phi(2,n-1;1,n;2,n)$, $\Delta\phi(3,n;1,n;5,n)$, $\Delta\phi(3,n;1,n;2,n)$, and $\Delta\phi(5,n;1,n;2,n)$. The elements of the vector $\phi(CH_3)_n$ in Eq. 3 are; $\Delta\phi(1,n;3,n;7,n)$, $\Delta\phi(1,n;3,n;8,n)$, $\Delta\phi(1,n;3,n;9,n)$, $\Delta\phi(8,n;3,n;9,n)$, $\Delta\phi(9,n;3,n;7,n)$, and $\Delta\phi(7,n;3,n;8,n)$. The elements of the vector $\phi(CH_2)_n$ in Eq. 5 are; $\Delta\phi(1,n;2,n;4,n)$, $\Delta\phi(1,n;2,n;6,n)$ $\Delta\phi(1,n;2,n;1,n+1)$, $\Delta\phi(4,n;2,n;6,n)$, $\Delta\phi(4,n;2,n;1,n+1)$, and $\Delta\phi(6,n;2,n;1,n+1)$, where $\Delta\phi$'s are the angle-bending coordinates for which the numbering of the atoms are shown in Fig. 1.

For the CH group of polypropylene, there are two CH bending modes. The CH bending

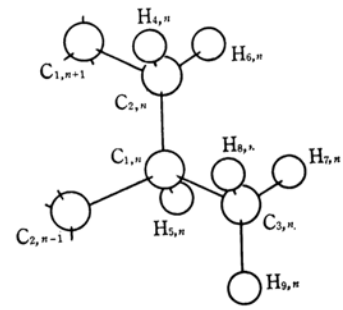

Fig. 1. Numbering of the carbon and hydrogen atoms of isotactic polypropylene chain (right-handed helix).

$$\begin{bmatrix} R_{1,n}\ (\text{CH bend.}^{ax}) \\ R_{2,n}\ (\text{CH bend.}^{eq}) \\ R_{3,n}\ (\delta^{s}) \\ R_{4,n}\ (\delta^{a}\ \text{ax.}) \\ R_{5,n}\ (\delta^{a}\ \text{eq.}) \end{bmatrix} = \begin{bmatrix} 0 & 1/6^{1/2} & 0 & 1/6^{1/2} & 0 & -2/6^{1/2} \\ 0 & -1/2^{1/2} & 0 & 1/2^{1/2} & 0 & 0 \\ 1/6^{1/2} & -1/6^{1/2} & 1/6^{1/2} & -1/6^{1/2} & 1/6^{1/2} & -1/6^{1/2} \\ -2/6^{1/2} & 0 & 1/6^{1/2} & 0 & 1/6^{1/2} & 0 \\ 0 & 0 & -1/2^{1/2} & 0 & 1/2^{1/2} & 0 \end{bmatrix} \phi(CH)_n \tag{1}$$

$$R_{6,n}\ (r_{CM}) = \Delta r(1,n;3,n) \tag{2}$$

$$\begin{bmatrix} R_{7,n}\ (CH_3\ \delta_a^{ax}) \\ R_{8,n}\ (CH_3\ \delta_a^{eq}) \\ R_{9,n}\ (CH_3\ \delta_s) \\ R_{10,n}\ (CH_3\ \text{rock.}^{ax}) \\ R_{11,n}\ (CH_3\ \text{rock.}^{eq}) \end{bmatrix} = \begin{bmatrix} 0 & 0 & 0 & 1/6^{1/2} & 1/6^{1/2} & -2/6^{1/2} \\ 0 & 0 & 0 & 1/2^{1/2} & -1/2^{1/2} & 0 \\ -1/6^{1/2} & -1/6^{1/2} & -1/6^{1/2} & 1/6^{1/2} & 1/6^{1/2} & 1/6^{1/2} \\ -1/6^{1/2} & -1/6^{1/2} & 2/6^{1/2} & 0 & 0 & 0 \\ -1/2^{1/2} & 1/2^{1/2} & 0 & 0 & 0 & 0 \end{bmatrix} \phi(CH_3)_n \tag{3}$$

$$R_{12,n}\ (r_{CC}^{ax}) = \Delta r(1,n;2,n) \tag{4}$$

$$\begin{bmatrix} R_{13,n}\ (\delta) \\ R_{14,n}\ (CH_2\ \text{bend.}) \\ R_{15,n}\ (CH_2\ \text{wag.}) \\ R_{16,n}\ (CH_2\ \text{twist.}) \\ R_{17,n}\ (CH_2\ \text{rock.}) \end{bmatrix} = \begin{bmatrix} 1/30^{1/2} & 1/30^{1/2} & -5/30^{1/2} & 1/30^{1/2} & 1/30^{1/2} & 1/30^{1/2} \\ 1/20^{1/2} & 1/20^{1/2} & 0 & -4/20^{1/2} & 1/20^{1/2} & 1/20^{1/2} \\ 1/2 & 1/2 & 0 & 0 & -1/2 & -1/2 \\ -1/2 & 1/2 & 0 & 0 & 1/2 & -1/2 \\ 1/2 & -1/2 & 0 & 0 & 1/2 & -1/2 \end{bmatrix} \phi(CH_2)_n \tag{5}$$

$$R_{18,n}\ (r_{CC}^{eq}) = \Delta r(2,n;1,n+1) \tag{6}$$

14) E. B. Wilson, Jr., *J. Chem. Phys.*, 7, 1047 (1939); 9, 76 (1941).

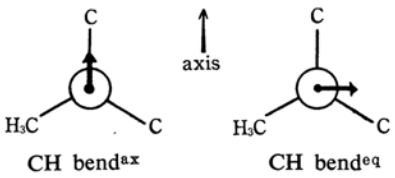

Fig. 2. The axial and equatorial CH bending modes.

mode in the axial direction (CH bend.^{ax}) and the bending mode in the equatorial direction (CH bend.^{eq}) (perpendicular to the helix axis) are given in Eq. 1 and are shown in Fig. 2. For the CH_3 group, there are two asymmetric deformation modes and two rocking modes. The asymmetric deformation mode in the axial direction (CH_3 δ_a^{ax}) and that in the equatorial direction (CH_3 δ_a^{eq}) and the rocking modes in the axial direction (CH_3 rock.^{ax}) and in the equatorial direction (CH_3 rock.^{eq}) are given in Eq. 3 and are shown in Fig. 3.

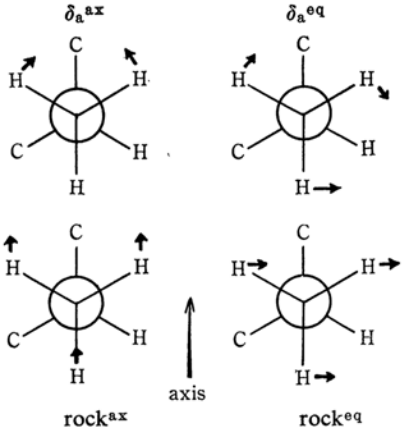

Fig. 3. The axial and equatorial CH_3 asymmetric deformation modes and rocking modes.

In deriving the potential energy matrix, $\boldsymbol{F}$, the modified Urey-Bradley force field[9] was used; the trans-coupling potential[10,11,15] for pairs of C–C–H bond angles in the trans arrangement, the gauche-coupling potential[11] for pairs of C–C–H angles in the gauche arrangement, and the l(C–C–H) angle interaction potential[10,11,16] for the CH_2 group were added as correction terms to the Urey-Bradley force field.[17]

The Urey-Bradley potential constants (in mdyn./Å) of K(C–H)=3.90 (CH group), K(C–H)=4.05 (CH_2 group), K(C–H)=4.05 (CH_3 group), F(H–C–H)=0.080 and F(H–C–C) =0.540 were used in correcting for the potential-energy interactions with high-frequency C–H stretching modes.[8]

The C–C stretching constants for the C-methyl bond and the main chain C–C bonds, the H–C–H bending constants for the CH_2 and CH_3 groups, the C–C–H bending constants for the CH, CH_2, and CH_3 groups, the C–C–C bending constant, the C···(C)···C repulsive constants, the intramolecular tension for the CH, CH_2, and CH_3 groups, the trans- and gauche-coupling constants and the angle-interaction constant (l) were adjusted by the

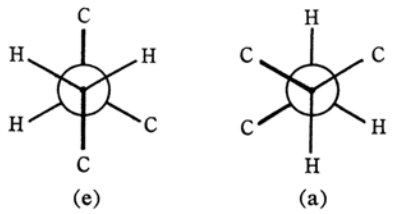

Fig. 4. Spatial arrangement of the carbon and hydrogen atoms of isotactic polypropylene chain (the right-handed helix); (e): as viewed along the equatorial C–C bond; (a): as viewed along the axial C–C bond. Main chain C–C bonds are drawn with heavy lines.

TABLE I. MODIFIED UREY-BRADLEY POTENTIAL CONSTANTS*1 OF ISOTACTIC POLYPROPYLENE AS ADJUSTED BY THE METHOD OF LEAST SQUARES

K(C–C)	2.11	Axial or equatorial C–C bond
	2.10	C-methyl bond
H(H–C–H)	0.414	CH_3 group
	0.393	CH_2 group
H(H–C–C)	0.222	CH_3 group
	0.205	CH_2 group
	0.225	CH group
H(C–C–C)	0.343	C–CH–C angle
	0.311	C–CH_2–C angle
F(H–C–H)	0.080*2	
F(H–C–C)	0.540*2	
F(C–C–C)	0.390	
κ	−0.027	CH_3 group
	0.028	CH_2 group
	−0.014	CH group
T	0.104	
G	−0.044	
l(C–C–H)	0.014	CH_2 group

*1 K, Stretching constant (in mdyn./Å); H, Bending constant (in mdyn./Å); F, Repulsive constant (in mdyn./Å); $F'=-F/10$; κ, Intramolecular tension (in mdyn·Å); T, Trans-coupling constant (in mdyn·Å); G, Gauche-coupling constant (in mdyn·Å); and l(C–C–H), Angle interaction constant (in mdyn·Å)

*2 Transferred from aliphatic hydrocarbons (Ref. 11).

15) J. Overend and J. R. Scherer, ibid., 35, 1681 (1960).
16) T. Shimanouchi and I. Suzuki, *J. Mol. Spectr.*, 6, 277 (1961).
17) T. Shimanouchi, *J. Chem. Phys.*, 17, 243, 734, 848 (1949).

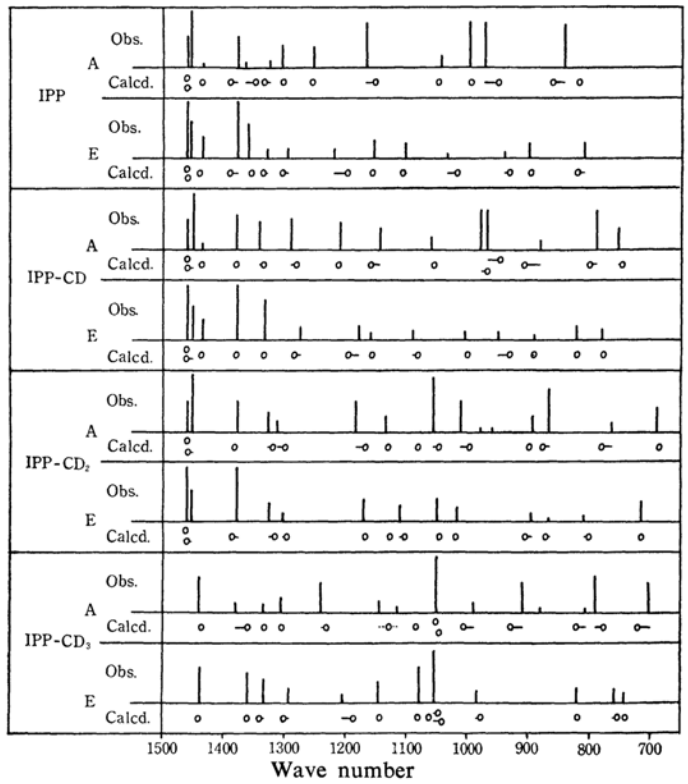

Fig. 5. Observed frequencies (cm^{-1}) and relative intensities (Ref. 1) and calculated frequencies of isotactic polypropylene [IPP], poly(propylene-2-d) [IPP-CD], poly(propylene-1, 1-d_2) [IPP-CD_2], and poly(propylene-3, 3, 3-d_3) [IPP-CD_3].

TABLE II. THE OBSERVED FREQUENCIES*1 (INTENSITY*2) AND THE CALCULATED FREQUENCIES (IN cm^{-1}) AND POTENTIAL ENERGY DISTRIBUTIONS*3 (IN %) OF THE A VIBRATIONS OF ISOTACTIC POLYPROPYLENE IN THE 1500～650 cm^{-1} REGION

ν_0	ν_c	Potential energy distributions
1460 (w)	1462 (ν_7)	CH_3 δ_a^{eq} (65), CH_3 δ_a^{ax} (15)
1454 (s)	1461 (ν_8)	CH_3 δ_a^{ax} (65), CH_3 δ_a^{eq} (20)
1435 (w)	1436 (ν_9)	CH_2 bend. (100)
1378*(m)	1390 (ν_{10})	CH_3 δ_s (65), CH bend. (15)
1365*(vw)	1348 (ν_{11})	CH_2 wag. (40), CH_3 δ_s (35), CH bend. (15)
1326 (w)	1334 (ν_{12})	CH bend.^{ax} (50), CH bend.^{eq} (25)
1304 (m)	1303 (ν_{13})	CH_2 wag. (45), CH_2 twist. (35), CH bend. (15)
1254 (m)	1256 (ν_{14})	CH_2 twist. (35), CH bend.^{ax} (15), CH bend.^{eq} (15)
1168 (s)	1152 (ν_{15})	r_{CC}^{ax} (40), CH_3 rock.^{ax} (20)
1045 (m)	1048 (ν_{16})	r_{CM} (45), r_{CC}^{eq} (30)
998 (s)	995 (ν_{17})	CH_3 rock.^{eq} (40), r_{CM} (25), CH bend. (20), CH_2 twist. (15)
973 (s)	951 (ν_{18})	CH_3 rock.^{ax} (50), r_{CC}^{ax} (25), r_{CC}^{eq} (20)
842 (s)	864 (ν_{19})	CH_3 rock. (30), r_{CC}^{eq} (20), r_{CM} (15)
	819 (ν_{20})	CH_2 rock. (70), CH bend. (20)

*1 The frequencies marked with * were observed by Tasumi and Shimanouchi (Ref. 20) and all the other frequencies were observed by Peraldo and Farina (Ref. 1).

*2 s: strong; m: medium; w: weak; and vw: very weak

*3 CH_3 δ_a, Methyl asymmetric deformation; CH_3 δ_s, Methyl symmetric deformation (see also Fig. 4), r_{CC}^{ax}, Axial C-C stretching; r_{CC}^{eq}; Equatorial C-C stretching; r_{CM}, C-methyl stretching mode.

TABLE III. THE OBSERVED FREQUENCIES*1 (INTENSITY*2) AND THE CALCULATED FREQUENCIES (IN cm^{-1}) POTENTIAL ENERGY DISTRIBUTIONS*3 (IN %) OF THE $E(2\pi/3)$ VIBRATIONS OF ISOTACTIC AND POLYPROPYLENE IN THE 1500~650 cm^{-1} REGION

ν_0	ν_c	Potential energy distributions
1460 (s)	1462 (ν_7)	CH_3 δ_a^{eq} (40), CH_3 δ_a^{ax} (40)
1454 (w)	1461 (ν_8)	CH_3 δ_a^{ax} (45), CH_3 δ_a^{eq} (40)
1435 (m)	1439 (ν_9)	CH_2 bend. (100)
1377 (s)	1390 (ν_{10})	CH_3 δ_s (70), CH bend.^{eq} (15)
1360 (m)	1356 (ν_{11})	CH bend.^{ax} (20), CH bend.^{eq} (15), CH_2 twist. (20), CH_2 wag. (15)
1330 (w)	1336 (ν_{12})	CH_2 wag. (45), CH bend.^{ax} (20), CH_3 δ_s (15)
1296 (w)	1304 (ν_{13})	CH_2 wag. (35), CH bend.^{eq} (25) CH bend.^{ax} (20)
1220 (w)	1197 (ν_{14})	CH_2 twist. (35), CH bend.^{ax} (15), r_{CC}^{eq} (15)
1155 (m)	1156 (ν_{15})	r_{CM} (20), CH bend. (15)
1103 (m)	1107 (ν_{16})	CH_3 rock. (ax : 20, eq : 10), r_{CC}^{ax} (25)
1034 (vw)	1017 (ν_{17})	r_{CM} (30), CH_2 twist. (20), CH bend. (15), CH_3 rock. (15)
941 (w)	931 (ν_{18})	CH_3 rock. (ax : 35, eq : 10), r_{CC}^{ax} (30), r_{CC}^{eq} (15)
899 (m)	896 (ν_{19})	CH_3 rock.^{eq} (40), CH_2 rock. (15), CH bend.^{eq} (15)
809 (m)	821 (ν_{20})	CH_2 rock. (35), r_{CM} (25), r_{CC}^{eq} (20)

*1 *2 *3 See *1 *2 *3 of Table II.

TABLE IV. THE OBSERVED FREQUENCIES*1 (INTENSITY*2) AND THE CALCULATED FREQUENCIES (IN cm^{-1}) AND POTENTIAL ENERGY DISTRIBUTIONS*3 (IN %) OF THE A VIBRATIONS OF ISOTACTIC POLY(PROPYLENE-2-D) IN THE 1500~650 cm^{-1} REGION

ν_0	ν_c	Potential energy distributions
1459 (w)	1459 (ν_7)	CH_3 δ_a^{eq} (85)
1451 (s)	1460 (ν_8)	CH_3 δ_a^{ax} (85)
1435 (w)	1436 (ν_9)	CH_2 bend. (100)
1379 (m)	1380 (ν_{10})	CH_3 δ_s (95)
1342 (m)	1336 (ν_{11})	CH_2 wag. (85)
1291 (m)	1279 (ν_{12})	CH_2 twist. (80)
1210 (m)	1212 (ν_{13})	r_{CC}^{ax} (30), r_{CC}^{eq} (25), CH_3 rock.^{ax} (15), CD bend. (ax : 15, eq : 10)
1145 (m)	1160 (ν_{14})	CH_3 rock. (25), CD bend. (25), r_{CM} (15)
1060 (w)	1054 (ν_{15})	CH_3 rock.^{eq} (30), CH_2 rock. (20)
981 (s)	968 (ν_{16})	r_{CM} (40), CH_3 rock.^{ax} (25), CD bend.^{ax} (20)
969 (s)	947 (ν_{17})	CH_3 rock. (ax : 25, eq : 10), r_{CC}^{ax} (20)
881 (w)	909 (ν_{18})	r_{CC}^{eq} (45), CD bend.^{eq} (20)
790 (s)	800 (ν_{19})	CD bend.^{eq} (30), CD bend.^{ax} (25), CH_3 rock. (eq : 20, ax : 10)
754 (m)	745 (ν_{20})	CH_2 rock. (55), CD bend.^{ax} (25), CD bend.^{eq} (25)

*1 *2 *3 See *1 *2 *3 of Table II.

TABLE V. THE OBSERVED FREQUENCIES*1 (INTENSITY*2) AND THE CALCULATED FREQUENCIES (IN cm^{-1}) AND POTENTIAL ENERGY DISTRIBUTIONS*3 (IN %) OF THE $E(2\pi/3)$ VIBRATIONS OF ISOTACTIC POLY(PROPYLENE-2-D) IN THE 1500~650 cm^{-1} REGION

ν_0	ν_c	Potential energy distributions
1459 (s)	1459 (ν_7)	CH_3 δ_a^{eq} (50), CH_3 δ_a^{ax} (35)
1451 (m)	1460 (ν_8)	CH_3 δ_a^{ax} (50), CH_3 δ_a^{eq} (35)
1435 (m)	1438 (ν_9)	CH_2 bend. (100)
1378 (s)	1380 (ν_{10})	CH_3 δ_s (95)
1334 (m)	1335 (ν_{11})	CH_2 wag. (85)
1273 (w)	1284 (ν_{12})	CH_2 twist. (55)
1179 (w)	1196 (ν_{13})	r_{CM} (20), r_{CC}^{eq} (15), CD bend. (15) CH_3 rock. (15)
1160 (vw)	1158 (ν_{14})	r_{CC}^{ax} (25), CH_3 rock.^{ax} (20), CH_2 twist. (15), CD bend. (15)
1091 (w)	1082 (ν_{15})	CH_3 rock.^{eq} (30), r_{CM} (15)
1005 (w)	1001 (r_{16})	CH_3 rock. (20), CH_2 rock. (20), CD bend. (15)
949 (w)	930 (ν_{17})	r_{CC}^{ax} (40), CH_3 rock. (ax : 30, eq : 10), r_{CC}^{eq} (15)
890 (vw)	891 (ν_{18})	CD bend. (ax : 35, eq : 10), r_{CM} (20), r_{CC}^{eq} (15)
821 (m)	820 (ν_{19})	CD bend. (eq : 35, ax : 10), r_{CM} (20), CH_3 rock.^{eq} (15)
781 (w)	775 (ν_{20})	CD bend.^{ax} (25), CD bend.^{eq} (25), CH_2 rock. (35)

*1 *2 *3 See *1 *2 *3 of Table II.

TABLE VI. THE OBSERVED FREQUENCIES*1 (INTENSITY*2) AND THE CALCULATED FREQUENCIES (IN cm^{-1}) AND POTENTIAL ENERGY DISTRIBUTION*3 (IN %) OF THE A VIBRATIONS OF ISOTACTIC POLY(PROPYLENE-1, 1-D_2) IN THE 1500～650 cm^{-1} REGION

ν_0	ν_c	Potential energy distributions
1461 (w)	1461 (ν_7)	CH_3 δ_a^{eq} (65), CH_3 δ_a^{ax} (20)
1452 (s)	1460 (ν_8)	CH_3 δ_a^{ax} (65), CH_3 δ_a^{eq} (20)
1377 (m)	1382 (ν_9)	CH_3 δ_s (90)
1327 (m)	1318 (ν_{10})	CH bend.^{eq} (55), CH bend.^{ax} (20)
1313 (w)	1301 (ν_{11})	CH bend.^{ax} (60), CH bend.^{eq} (15)
1184 (s)	1167 (ν_{12})	r_{CC}^{ax} (45), CD_2 wag. (20)
1134 (m)	1130 (ν_{13})	CH_3 rock.^{eq} (20), CD_2 twist. (15)
	1082 (ν_{14})	r_{CM} (25), r_{CC}^{eq} (20), CH_3 rock.^{ax} (20)
1058 (s)	1048 (ν_{15})	CD_2 bend. (60), CH_3 rock.^{eq} (15)
1013 (s)	997 (ν_{16})	r_{CM} (30), CD_2 wag. (25), r_{CC}^{eq} (20), CH_3 rock.^{ax} (20)
894 (m)	900 (ν_{17})	CH_3 rock. (eq : 20, ax : 10), CD_2 wag. (20), CD_2 twist. (20)
868 (s)	878 (ν_{18})	CH_3 rock.^{ax} (25), CH_3 rock.^{eq} (20), CD_2 twist. (15), CH bend. (15)
764 (w)	782 (ν_{19})	CD_2 twist. (40), r_{CC}^{eq} (20), r_{CM} (15)
691 (m)	688 (ν_{20})	CD_2 rock. (80)

*1 *2 *3 See *1 *2 *3 of Table II.

TABLE VII. THE OBSERVED FREQUENCIES*1 (INTENSITY*2) AND THE CALCULATED FREQUENCIES (IN cm^{-1}) AND POTENTIAL ENERGY DISTRIBUTIONS*3 (IN %) OF THE E($2\pi/3$) VIBRATIONS OF ISOTACTIC POLY(PROPYLENE-1, 1-D_2) IN THE 1500～650 cm^{-1} REGION

ν_0	ν_c	Potential energy distributions
1461 (s)	1462 (ν_7)	CH_3 δ_a^{eq} (75)
1452 (m)	1460 (ν_8)	CH_3 δ_a^{ax} (80)
1377 (s)	1386 (ν_9)	CH_3 δ_s (85)
1325 (m)	1314 (ν_{10})	CH bend.^{eq} (50), CH bend.^{ax} (15), CH_3 δ_s (20)
1303 (w)	1296 (ν_{11})	CH bend.^{ax} (65), CH bend.^{eq} (20)
1170 (m)	1168 (ν_{12})	r_{CC}^{eq} (35), CD_2 bend. (15)
	1128 (ν_{13})	r_{CC}^{ax} (30), CD_2 wag. (15), r_{CM} (15), CH_3 rock. (15)
1110 (m)	1103 (ν_{14})	CD_2 wag. (20), CH_3 rock.^{eq} (20)
1051 (m)	1043 (ν_{15})	CD_2 bend. (70)
1018 (m)	1020 (ν_{16})	CD_2 wag. (35), CH_3 rock.^{ax} (25), r_{CM} (20)
896 (w)	904 (ν_{17})	CH_3 rock.^{eq} (25), CH_3 rock.^{ax} (15), r_{CC}^{ax} (20)
868 (w)	868 (ν_{18})	CH_3 rock.^{ax} (20), CH_3 rock.^{eq} (20), r_{CC}^{ax} (15), CD_2 twist. (15)
811 (w)	801 (ν_{19})	CD_2 twist. (65)
715 (m)	715 (ν_{20})	CD_2 rock. (45), r_{CM} (15), r_{CC}^{eq} (15)

*1 *2 *3 See *1 *2 *3 of Table II.

TABLE VIII. THE OBSERVED FREQUENCIES*1 (INTENSITY*2) AND THE CALCULATED FREQUENCIES (IN cm^{-1}) AND POTENTIAL ENERGY DISTRIBUTIONS*3 (IN %) OF THE A VIBRATIONS OF ISOTACTIC POLY(PROPYLENE-3, 3, 3-D_3) IN THE 1500～650 cm^{-1} REGION

ν_0	ν_c	Potential energy distributions
1440 (m)	1436 (ν_7)	CH_2 bend. (100)
1379 (w)	1359 (ν_8)	CH_2 wag. (50), CH bend.^{eq} (30)
1334 (w)	1333 (ν_9)	CH bend.^{ax} (55), CH bend.^{eq} (25)
1305 (m)	1304 (ν_{10})	CH_2 wag. (40), CH_2 twist. (35), CH bend. (15)
1239 (m)	1230 (ν_{11})	CH_2 twist. (35), CH bend.^{ax} (25), CH bend.^{eq} (25)
1145 (w)	1128 (ν_{12})	r_{CC}^{ax} (55)
1115 (w)	1083 (ν_{13})	CD_3 δ_s (65), r_{CM} (50)
1051 (s)	1049 (ν_{14})	CD_3 δ_a^{ax} (45), CD_3 δ_a^{eq} (40)
	1045 (ν_{15})	CD_3 δ_a^{ax} (50), CD_3 δ_a^{eq} (40)
989 (w)	1006 (ν_{16})	r_{CC}^{eq} (35), CD_3 δ_s (25)
909 (m)	928 (ν_{17})	r_{CM} (20), r_{CC}^{eq} (15), CD_3 rock.^{eq} (15), CH_2 twist. (15)
807 (vw)	820 (ν_{18})	CH_2 rock. (70), r_{CM} (15)
791 (s)	775 (ν_{19})	CD_3 rock.^{ax} (40), CD_3 rock.^{eq} (25)
703 (m)	720 (ν_{20})	CD_3 rock.^{eq} (40), CD_3 rock.^{ax} (30)

*1 *2 *3 See *1 *2 *3 of Table II.

TABLE IX. THE OBSERVED FREQUENCIES*1 (INTENSITY*2) AND THE CALCULATED FREQUENCIES (IN cm^{-1}) AND POTENTIAL ENERGY DISTRIBUTIONS*3 (IN %) OF THE $E(2\pi/3)$ VIBRATIONS OF ISOTACTIC POLY(PROPYLENE-3, 3, 3-D_3) IN THE 1500~650 cm^{-1} REGION

ν_0	ν_c	Potential energy distributions
1438 (s)	1439 (ν_7)	CH_2 bend. (100)
1361 (m)	1361 (ν_8)	CH bend. (eq: 30, ax: 10), CH_2 wag. (20), CH_2 twist. (25)
1333 (m)	1339 (ν_9)	CH_2 wag. (45), CH bend.^{ax} (35)
1293 (m)	1299 (ν_{10})	CH_2 wag. (35), CH bend.^{eq} (30), CH bend.^{ax} (25)
1206 (w)	1184 (ν_{11})	CH_2 twist. (35), CH bend.^{ax} (15), r_{CC}^{eq} (15)
1145 (m)	1143 (ν_{12})	r_{CM} (30), CH bend. (15)
1081 (m)	1079 (ν_{13})	r_{CC}^{ax} (35), CD_3 δ_s (15), r_{CC}^{eq} (15)
	1061 (ν_{14})	CD_3 δ_s (55), CD_3 δ_a (20)
1054 (s)	1044 (ν_{15})	CD_3 δ_a^{eq} (70), CD_3 δ_a^{ax} (15)
	1040 (ν_{16})	CD_3 δ_a^{ax} (55), CD_3 δ_a^{eq} (20)
984 (w)	976 (ν_{17})	CH_2 rock. (15), r_{CM} (15)
821 (m)	818 (ν_{18})	CH_2 rock. (30), r_{CM} (20), r_{CC}^{eq} (15)
759 (m)	753 (ν_{19})	CD_3 rock.^{ax} (35), CD_3 rock.^{eq} (30)
743 (w)	739 (ν_{20})	CD_3 rock.^{eq} (40), CD_3 rock.^{ax} (25)

*1 *2 *3 See *1 *2 *3 of Table II.

TABLE X. THE OBSERVED*1 AND CALCULATED FREQUENCIES BELOW 650 cm^{-1} AND THE CALCULATED POTENTIAL ENERGY DISTRIBUTIONS (IN %)*2 OF ISOTACTIC POLYPROPYLENE [IPP], POLY(PROPYLENE-2-D) [IPP-CD], POLY(PROPYLENE-1, 1-D_2) [IPP-CD_2] AND POLY(PROPYLENE-3, 3, 3-D_3) [IPP-CD_3]

	IPP			ν_c	
ν_0	ν_c	Potential energy distributions	IPP-CD	-CD_2	-CD_3
528	514 (ν_{21}^E)	δ^a (35), δ (25)	498	488	490
460	435 (ν_{22}^E)	δ^s (70)	428	391	407
456	479 (ν_{21}^A)	δ^a (75)	470	453	445
398	391 (ν_{22}^A)	δ^s (45), δ^a (30)	387	371	360
321	309 (ν_{23}^E)	δ^a (65)	307	293	285
251	260 (ν_{23}^A)	δ^a (45), δ^s (30)	257	238	248
	138 (ν_{24}^E)	δ^a (55), δ (45)	137	131	127
	118 (ν_{24}^A)	δ (50), δ^a (20)	114	110	110

*1 Observed in previous studies (Refs. 8 and 12). Only the frequencies above 250 cm^{-1} are listed for comparisons.

*2 δ^s and δ^a, the symmetric and asymmetric deformations, respectively, of the CH_2-$CH(CH_3)$-CH_2 group; δ, the C-CH_2-C deformation.

method of least squares.[18] The initial set of these constants as transferred from ethane, propane, and isobutane[11] have been described previously[8]. All the fundamental frequencies of $[-CH_2-CH(CH_3)-]_n$, $[-CH_2-CD(CH_3)-]_n$, $[-CD_2-CH(CH_3)-]_n$, and $[-CH_2-CH(CD_3)-]_n$ observed by Peraldo and Farina[1] in the 1500~650 cm^{-1} region and the skeletal frequencies of $[-CH_2-CH(CH_3)-]_n$[8,12] (A species: 456, 398 and 251 cm^{-1}; $E(2\pi/3)$ species: 528, 460 and 321 cm^{-1}) were used for the adjustment of potential constants. The potential constants thus obtained are shown in Table I. A common stretching constant K(C-C) was used for the axial C-C bond and for the equatorial C-C bond since the arrangements of the carbon and hydrogen atoms adjacent to these C-C bonds are the same, as Fig. 4 shows. In the adjustments of the potential constants, the elements of Jacobian matrices (derivatives of frequencies with respect to potential constants) were calculated by means of an equation reported previously.[19]

The trans-coupling ($T=0.104$) and gauche-coupling ($G=-0.044$) constants of polypropylene agree closely with the corresponding constants for polyethylene ($T=0.100$ and $G=-0.033$) and for ethane ($T=0.107$ and $G=-0.025$).[9] It is interesting to note that the gauche constant is nearly equal to $-T/2$.

The frequencies calculated with the final set of potential constants may be compared

18) D. E. Mann, T. Shimanouchi, J. H. Meal and L. Fano, *J. Chem. Phys.*, **27**, 43 (1957).

19) T. Miyazawa, *J. Chem. Soc. Japan, Pure Chem. Sec. (Nippon Kagaku Zasshi)*, **76**, 1132 (1955).

TABLE XI. THE L MATRIX ELEMENTS FOR THE A VIBRATIONS OF ISOTACTIC POLYPROPYLENE IN THE 1500～650 cm^{-1} REGION

S_i*	ν_7 1462	ν_8 1461	ν_9 1436	ν_{10} 1390	ν_{11} 1348	ν_{12} 1334	ν_{13} 1303	ν_{14} 1256	ν_{15} 1152	ν_{16} 1048	ν_{17} 995	ν_{18} 951	ν_{19} 864	ν_{20} 819
CH bend.^{ax}	−1	1	1	2	−3	9	3	−5	2	−1	−3	1	2	2
CH bend.^{eq}	−2	−1	1	5	−4	−7	4	−4	0	3	−3	0	1	−3
δ^s	0	0	0	0	0	0	1	2	1	1	−2	0	−2	1
δ^a (ax)	0	0	0	−1	1	−1	0	0	3	1	1	0	−1	0
δ^a (eq)	0	0	0	1	−1	−1	−1	0	0	−1	−1	1	0	0
r_{CM}	0	0	0	0	2	0	0	0	0	3	2	0	1	1
CH_3 δ_a^{ax}	−6	13	−2	−1	1	−2	0	2	2	0	0	2	1	0
CH_3 δ_a^{eq}	12	7	1	2	−1	−2	0	−3	1	−1	2	1	−1	0
CH_3 δ_s	−1	0	0	11	8	1	−1	1	0	1	1	0	0	0
CH_3 rock.^{ax}	2	−4	0	0	0	−1	−1	2	5	−1	−1	6	3	−1
CH_3 rock.^{eq}	−4	−2	0	0	−1	−1	0	−4	2	−2	6	2	−3	2
r_{CC}^{ax}	0	0	0	1	−1	1	−1	−1	−3	0	0	2	1	0
δ	0	0	−1	0	0	1	−1	−1	−2	−1	1	0	2	−1
CH_2 bend.	−1	1	15	−1	1	0	0	0	0	0	0	0	0	0
CH_2 wag.	1	0	−1	−4	8	−2	8	−2	0	−2	−1	0	0	0
CH_2 twist.	0	0	0	2	−3	1	7	7	−1	−1	4	−1	1	0
CH_2 rock.	0	0	0	1	−1	−3	0	0	−1	−2	−1	0	2	6
r_{CC}^{eq}	0	0	0	0	0	−1	0	−1	1	−2	0	−2	1	−1

* For the notation of the symmetry coordinates, see *3 of Table II.

with the observed frequencies in Tables II—X and in Fig. 5. Except for the unobserved fundamentals, the r. m. s. frequency deviations for the vibrations lying in the 1500～650 cm^{-1} region are: $[-CH_2-CH(CH_3)-]_n$: 1.0%, $[-CH_2-CD(CH_3)-]_n$: 1.1%, $[-CD_2-CH(CH_3)-]_n$: 1.0%, and $[-CH_2-CH(CD_3)-]_n$: 1.2%, and the overall deviation is 1.1%. In view of the small number (a total of 16) of potential constants as compared with the large number (a total of 108) of observed frequencies, a frequency deviation as small as this indicates that these potential constants may now be used for the elucidation of the nature of observed fundamental vibrations. Therefore, the potential energy distributions ($F_{ii}L_{ip}^2/4\pi^2c^2\nu^2$) were also calculated as shown in Tables II–X for the A and E($2\pi/3$) vibrations of polypropylene and the deuterated derivatives. Only the terms greater than 15% are listed in Tables II–X.

For nondegenerate vibrations, the normal modes may be expressed by the elements of the L matrix. When the p-th normal vibration is excited, the i-th internal coordinate (or local symmetry coordinate) of the n-th repeating unit is given by

$$R_{i,n}=(1/N)^{1/2}L_{ip}Q_p \qquad (7)$$

where Q_p is the normal coordinate for the p-th vibration and $(1/N)^{1/2}$ is the normalization factor. On the other hand, for degenerate vibrations of a helical molecule associated with the phase difference of δ, the normal modes may be expressed by the amplitude factor $L_{ip}(\delta)$ and the phase angle $\varepsilon_{ip}(\delta)$. When the p-th degenerate vibration is excited, the i-th internal coordinate of the n-th unit is given by:

$$R_{i,n}=(2/N)^{1/2}L_{ip}(\delta)\{Q_{pa}(\delta)\cos[n\delta+\varepsilon_{ip}(\delta)] + Q_{pb}(\delta)\sin[n\delta+\varepsilon_{ip}(\delta)]\} \qquad (8)$$

where $Q_{pa}(\delta)$ and $Q_{pb}(\delta)$ are the p-th pair of normal coordinates with the phase difference of δ.[8] The L matrix elements [in units of 1/10·Å·(atomic weight)$^{1/2}$] for the A vibrations of isotactic polypropylene are listed in Table XI. The amplitude factor [in units of 1/10·Å·(atomic weight)$^{1/2}$] and the phase angle (in degrees) for the E($2\pi/3$) vibrations are listed in Table XII, where the phase angles were taken in the range of $+90°$～$-90°$ with the result that the values of a number of L_{ip}'s were taken to be negative.

CH_2 Bending Vibrations

The band of polypropylene at 1435 cm^{-1} is also observed for $[-CH_2-CD(CH_3)-]_n$ and $[-CH_2-CH(CD_3)-]_n$, but not for $[-CD_2-CH(CH_3)-]_n$. This band is assigned to the CH_2 bending vibration.[1,4] As is shown in Tables II—V, VIII and IX, the potential energy of this vibration is almost exclusively associated with the CH_2 bending mode.

For $[-CH_2-CH(CD_3)-]_n$, the bands due to the A and E components have been resolved at 1440 (parallel: ∥) and 1438 cm^{-1} (perpendicular: ⊥), respectively.[1] The infrared

20) M. Tasumi and T. Shimanouchi (private communication).

TABLE XII. THE AMPLITUDE FACTORS AND PHASE ANGLES*1 FOR THE $E(2\pi/3)$ VIBRATIONS OF ISOTACTIC POLYPROPYLENE IN THE 1500~650 cm^{-1} REGION

S_i*2	ν_7 1462	ν_8 1461	ν_9 1439	ν_{10} 1390	ν_{11} 1356	ν_{12} 1336	ν_{13} 1304	ν_{14} 1197	ν_{15} 1156	ν_{16} 1107	ν_{17} 1017	ν_{18} 931	ν_{19} 896	ν_{20} 821
CH bend.^{ax}	−1 (0)	1 (−5)	1 (−25)	1 (−5)	6 (0)	5 (0)	−6 (−75)	−4 (5)	−3 (60)	2 (80)	1 (45)	1 (−20)	−1 (25)	2 (25)
CH bend.^{eq}	−1 (0)	−1 (0)	−1 (−50)	5 (0)	−5 (−5)	3 (35)	6 (45)	3 (−15)	3 (0)	2 (−75)	−2 (−45)	−1 (−80)	−3 (−15)	1 (−55)
δ^s	0	0	0	0	0	1 (−80)	−1 (−35)	2 (60)	−2 (60)	−1 (85)	−2 (−60)	0	1 (15)	0
δ^a (ax)	0	0	0	0	−1 (0)	−1 (25)	−1 (35)	1 (−80)	1 (−40)	2 (15)	0	−1 (65)	0	0
δ^a (eq)	0	0	1 (−20)	1 (5)	−1 (5)	1 (20)	0	1 (−85)	−2 (5)	1 (45)	−1 (30)	−1 (−40)	−1 (25)	−1 (60)
r_{CM}	0	0	0	0	1 (−10)	−1 (20)	−1 (55)	0	2 (0)	1 (−15)	2 (0)	0	−1 (25)	−2 (−35)
CH_3 δ_a^{ax}	−10 (0)	10 (0)	−1 (5)	−1 (−5)	−2 (−5)	−2 (20)	−2 (55)	1 (−10)	−1 (40)	2 (−5)	−1 (−75)	2 (0)	−1 (15)	0
CH_3 δ_a^{eq}	10 (0)	10 (0)	0	2 (5)	−2 (10)	2 (40)	2 (35)	−2 (70)	1 (60)	1 (25)	1 (−85)	1 (−30)	2 (−10)	0
CH_3 δ_s	−1 (5)	0	0	12 (0)	5 (−5)	−6 (10)	−3 (65)	0	1 (0)	0	1 (−5)	0	0	0
CH_3 rock.^{ax}	3 (0)	−3 (0)	0	0	−1 (0)	−1 (25)	−2 (50)	1 (−25)	−3 (40)	5 (0)	−2 (−65)	5 (0)	−2 (10)	1 (35)
CH_3 rock.^{eq}	−3 (0)	−3 (0)	0	1 (5)	−1 (10)	1 (45)	2 (30)	−4 (75)	2 (45)	3 (25)	3 (−80)	3 (−30)	5 (0)	0
r_{CC}^{ax}	0	0	0	0	1 (−35)	1 (−20)	0	−1 (−25)	1 (75)	−2 (10)	−1 (50)	2 (−20)	−1 (−5)	−1 (−80)
δ	0	0	−1 (5)	−1 (20)	0	−1 (55)	−1 (85)	−1 (−70)	3 (25)	0	1 (40)	1 (−25)	0	1 (65)
CH_2 bend.	−1 (−35)	1 (0)	15 (0)	0	−2 (30)	−1 (0)	0	0	1 (35)	0	0	0	0	0
CH_2 wag.	−1 (90)	0	0	−5 (−20)	5 (25)	−8 (−55)	7 (0)	−2 (−85)	−1 (10)	2 (20)	−1 (−50)	0	0	0
CH_2 twist.	0	1 (20)	1 (0)	−2 (60)	6 (30)	3 (−50)	−1 (−45)	6 (0)	2 (60)	3 (−25)	−4 (50)	−1 (−15)	−1 (−45)	0
CH_2 rock.	0	0	0	−1 (65)	−1 (−50)	−1 (5)	2 (−60)	−4 (80)	−3 (−85)	−2 (−75)	2 (−25)	−1 (−15)	−3 (40)	4 (0)
r_{CC}^{eq}	0	0	0	−1 (45)	1 (55)	0	0	−1 (50)	1 (45)	1 (−75)	1 (85)	1 (65)	1 (15)	1 (25)

*1 Phase angles are listed in parentheses. *2 For the notation of the symmetry coordinates, see *3 of Table II.

intensity ratio for these CH_2 bending vibrations has been calculated to be A : E = 1.8 : 1,[21] where the C-C-C bond angle has been assumed to be 114.5°.*2 In fact, the parallel peak at 1440 cm^{-1} has been found to be slightly stronger than the perpendicular peak at 1438 cm^{-1} (Fig. 4f of Ref. 1).

For neither $[-CH_2-CH(CH_3)-]_n$ nor $[-CH_2-CD(CH_3)-]_n$ has the band at 1435 cm^{-1} been resolved into two components. Furthermore, the calculated frequencies of the A and E CH_2 bending vibrations are essentially the same. Accordingly, the strong ⊥ dichroism of the band at 1435 cm^{-1} indicates that the E vibration is appreciably stronger than the A vibration; the observed ratio (A : E) is very different from the ratio estimated from the spatial structure or from the ratio observed for $[-CH_2-CH(CD_3)-]_n$. Since the spatial structure of isotactic polypropylene will not change much upon isotopic substitution, the appreciably weak relative intensity of the A component is possibly associated with the normal mode (or hybridization). It may be seen in Tables XI and XII that the hybridization of the methyl asymmetric deformation mode is greater for the CH_2 bending vibration (ν_9) of the A species than the corresponding ν_9 vibration of the E species. For $[-CH_2-CH(CH_3)-]_n$ and $[-CH_2-CD(CH_3)-]_n$, the asymmetric deformation frequencies of the methyl group lie within 30 cm^{-1} of the CH_2 bending frequency and so slight hybridization may well be expected, even though the methyl group is separated from the CH_2 group by the CH group. The slight coupling of the CH_2 bending mode and the CH_3 asymmetric deformation modes is also suggested from the higher frequency shift of the CH_2 bending band upon the deuteration of the CH_3 group.

CH_3 Deformation Vibrations

Asymmetric Deformation Modes. — The ∥ band at 1454 cm^{-1} and the ⊥ band at 1460 cm^{-1} of polypropylene are also observed for $[-CH_2-CD(CH_3)-]_n$ and $[-CD_2-CH(CH_3)-]_n$, but not for $[-CH_2-CH(CD_3)-]_n$. These bands are assigned to the asymmetric deformation vibrations of the CH_3 group.[1,4,6] The calculated A and E frequencies (ν_7 and ν_8) are nearly the same. Neither the band at 1460 nor that at 1454 cm^{-1} has been resolved into two components, and the dichroism is not strong. Apparently, the 1460 cm^{-1} (⊥) band due to the E vibration is overlapped by the corresponding ∥ band due to the A vibration, and the 1454 cm^{-1} (∥) band due to the A vibration is overlapped by the corresponding ⊥ band due to the E vibration.

Symmetric Deformation Modes. — The ⊥ band of $[-CH_2-CH(CH_3)-]_n$ at 1377 cm^{-1} is also observed for $[-CH_2-CD(CH_3)-]_n$ and $[-CD_2-CH(CH_3)-]_n$ but not for $[-CH_2-CH(CD_3)-]_n$.*3 This band is assigned to the CH_3 symmetric deformation vibration. The frequencies calculated for the corresponding A and E vibrations are essentially the same. Accordingly, the perpendicular dichroism of the band at 1377 cm^{-1} indicates that the perpendicular band due to the E vibration is stronger than the parallel band due to the A vibration. The intensity ratio of the A and E bands has been estimated by Krimm[21] to be 0.4 : 1.0, a figure in good agreement with the observed intensity ratio.

The Normal Vibrations of Polypropylene $[-CH_2-CH(CH_3)-]_n$

In our previous study, the normal vibrations of isotactic polypropylene were treated by the use of potential constants as transferred from other hydrocarbons[8]. In the present study, the gauche-coupling potential and the l(C-C-H) potential were introduced, and the potential constants were refined by the method of least squares. Therefore, the potential energy distributions calculated in the present study differ somewhat from the previous ones. In the following discussions, the nature of the normal vibrations will be discussed, referring to the potential energy distributions as listed in Tables II—IX and to the normal modes as listed in Tables XI and XII.

CH_2 Wagging and Twisting Modes and CH Bending Mode.—In the region between 1370 and 1200 cm^{-1}, four parallel bands (1365, 1326, 1304, and 1254 cm^{-1}) and four perpendicular bands (1360, 1330, 1296, and 1220 cm^{-1}) have been observed for $[-CH_2-CH(CH_3)-]_n$. Similar spectra have also been observed for $[-CH_2-CH(CD_3)-]_n$, but not for either $[-CH_2-CD(CH_3)-]_n$ or $[-CD_2-CH(CH_3)-]_n$. As is shown in Tables II, III, XI, and XII, these bands of $[-CH_2-CH(CH_3)-]_n$ arise from the hybridized vibrations of the CH_2 wagging and twisting modes and from those of the axial and equatorial CH bending modes.

Upon the deuteration of the CH group, two parallel bands (at 1342 and 1291 cm^{-1}) and two perpendicular bands (1334 and 1273 cm^{-1}) have been observed for $[-CH_2-CD(CH_3)-]_n$.

21) S. Krimm, *Fortschr. Hochpolymer.-Forsch.*, 2, 51 (1960).

*2 If the C-C-C bond angle is assumed to have the tetrahedral value, the intensity ratio is derived as A : E = 1 : 1.

*3 As will be discussed later, the parallel band of $[-CH_2-CH(CD_3)-]_n$ at 1379 cm^{-1} is assigned to the ν_8^A vibration (see Table VIII).

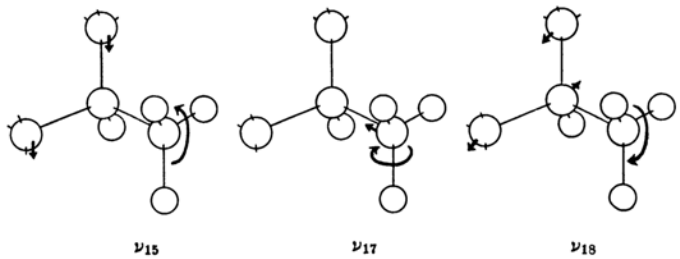

Fig. 6. Schematic representations of the normal modes of the ν_{15}, ν_{17} and ν_{18} vibrations (A species) of isotactic polypropylene.

These bands are due to the CH_2 wagging and twisting modes, which are not hybridized with the CH bending modes (Tables IV and V). On the other hand, for $[-CD_2-CH(CH_3)-]_n$, two parallel bands (1327 and 1313 cm^{-1}) and two perpendicular bands 1325 and 1303 cm^{-1}) have been observed[1] (Tables VI and VII). These bands arise from the CH bending modes (axial and equatorial), which are not hybridized with either the CH_2 wagging or twisting modes. It is interesting to note that the 'intrinsic' CH_2 wagging and twisting frequencies observed for $[-CH_2-CD(CH_3)-]_n$, as well as the 'intrinsic' CH bending frequencies observed for $[-CD_2-CH(CH_3)-]_n$, all lie in the narrow region of 1350~1270 cm^{-1}. Naturally the CH_2 wagging and twisting modes and the CH bending modes are extensively hybridized for the molecule of $[-CH_2-CH(CH_3)-]_n$.

In our previous study, the weak $\parallel$ band at 1254 cm^{-1} and the weak $\perp$ band at 1220 cm^{-1} were considered to arise primarily from the CH_2 twisting modes. Actually, however, these frequencies are much lower than the 'intrinsic' CH_2 twisting frequencies as observed for $[-CH_2-CD(CH_3)-]_n$. The A vibration at 1254 cm^{-1} is due to the CH_2 twisting mode as coupled with the CH bending mode in the H–C–methyl plane, whereas the E vibration at 1220 cm^{-1} is due to the CH_2 twisting mode as coupled with the CH bending mode perpendicular to the H–C–methyl plane.

CH_3 and CH_2 Rocking Modes and C–C Stretching Modes.—In the region between 1200 and 900 cm^{-1}, five strong parallel bands due to the A vibrations and five perpendicular bands due to the E vibrations are observed. As Tables II, III, XI, and XII show, these bands of polypropylene arise from the hybridized vibrations of the axial and equatorial CH_3 rocking, the axial and equatorial C–C stretching, the C–methyl stretching, and the CH_2 rocking modes.*5

The parallel bands at 1168, 998, 973 and 842 cm^{-1} are the strongest peaks of polypropylene. As Table II shows, all these bands are associated with the methyl rocking modes. However, the hybridization of the C–C stretching modes is appreciable for these vibrations. Thus, the band at 1168 cm^{-1} is primarily associated with the axial C–C stretching mode as coupled with the axial methyl rocking mode. The band at 1045 cm^{-1} is due to the asymmetric stretching mode of the C-methyl bond and the equatorial C–C bond. The band at 998 cm^{-1} is due to the equatorial rocking mode coupled with the C-methyl bond, whereas the band at 973 cm^{-1} is due to the axial rocking mode as coupled with the antisymmetric stretching mode of the axial and equatorial C–C bonds. The band at 842 cm^{-1} is associated with the methyl rocking mode in the H–C-methyl plane coupled with the symmetric stretching mode of the C-methyl and the equatorial C–C bonds. The hybridizations of the C–C stretching modes and the methyl rocking modes are schematically shown in Fig. 6 for the A vibrations at 1168, 998 and 973 cm^{-1}.

It might be anticipated that the intensities of the parallel bands at 1168 and 973 cm^{-1} are due to the methyl rocking modes in the axial direction. However, the intensity of the band at 998 cm^{-1} is as strong as those of the bands at 1168 or 973 cm^{-1}, although the vibration at 998 cm^{-1} is largely associated with the equatorial methyl rocking mode. Apparently more extensive studies are necessary for a detailed discussion of the intensities of bands arising from much hybridized modes.

*4 The assignments by Liang et al.[4] were: 1360 ($\perp$), 1330 ($\perp$), CH_2 wag.+CH bend.; 1304 ($\parallel$) and 1296 ($\perp$), CH_2 twist.+CH and CH_3 bend.; 1255 ($\parallel$) and 1220 cm^{-1} ($\perp$), CH bend.+CH_2 rock.+CH_3 rock. The assignments by McDonald and Ward[6] were: 1360 ($\perp$), 1304 ($\parallel$), 1254 ($\parallel$), and 1220 ($\perp$), CH bend.; 1330 ($\perp$), CH_2 wag.; and 1296 cm^{-1} ($\perp$), CH_2 twist.

*5 The assignments by Liang et al.[4] were: 1168 ($\parallel$) and 1155 ($\perp$), CH_3 rock.+CH_2 and CH bend.; 1103 ($\perp$), 1045 ($\parallel$), 998 ($\parallel$), 941 ($\parallel$) and 899 ($\perp$), r_{CC}; 973 ($\parallel$), CH_3 rock.+CH_2 and CH rock.; 840 ($\parallel$) and 809 ($\perp$), CH_2 rock.+CH and CH_3 rock. The assignments by McDonald and Ward[6] were: 1168 ($\parallel$), CH_3 rock.+r_{CC}; 1103 ($\perp$), 941 ($\perp$), 899 ($\perp$) and 809 ($\perp$), CH bend.+r_{CC}; 1045 ($\parallel$), r_{CC}+CH_3 rock.; 998 ($\parallel$), r_{CC}+CH_3 rock.+CH_2 rock.; 973 ($\parallel$), CH_3 rock.+CH_2 rock.+r_{CC}; 842 ($\parallel$), CH_2 rock.+CH_3 rock.+r_{CC}.

The perpendicular band of polypropylene at 1155 cm^{-1} has also been observed in the Raman effect[22]. This band corresponds to the calculated ν_{15}^{E} frequency of 1156 cm^{-1}. Although the ν_{15}^{E} perpendicular band and the ν_{15}^{A} parallel band lie close to each other, these vibrations are quite different from each other. Thus the ν_{15}^{E} vibration is primarily associated with the C-methyl stretching mode as coupled with the CH bending modes modes in the axial and equatorial directions, but it is not much associated with the methyl rocking modes. On the other hand, the three perpendicular bands at 1103, 941 and 899 cm^{-1} are due to the methyl rocking modes, where the contributions of the axial or equatorial C–C stretching modes are also appreciable.

The band at 1103 cm^{-1} is due to the methyl rocking mode in the axial direction ($\varepsilon=0°$), the rocking mode in the equatorial direction ($\varepsilon=25°$), and the axial C–C stretching mode ($\varepsilon=10°$), with small phase angle differences among them. The band at 941 cm^{-1} is due to the axial methyl rocking mode ($\varepsilon=0°$), the equatorial rocking mode ($\varepsilon=-30°$), the axial C–C stretching mode ($\varepsilon=-20°$), and the equatorial C–C stretching mode ($\varepsilon=65°$). The axial and equatorial C–C stretching modes for this vibration are almost 90° out-of-phase. The band at 899 cm^{-1} is due to the equatorial methyl rocking mode ($\varepsilon=0°$), the equatorial CH bending mode ($\varepsilon=-15°$), and the CH_2 rocking mode ($\varepsilon=40°$), all of which take place in the equatorial direction. The methyl rocking mode and the CH bending mode are almost in phase for this vibration.

The perpendicular band at 809 cm^{-1} is due to the CH_2 rocking mode ($\varepsilon=0°$), coupled with the C-methyl stretching mode ($\varepsilon=-35°$) and the equatorial C–C stretching mode ($\varepsilon=25°$). On the other hand, the ν_{20}^{A} vibration calculated at 819 cm^{-1} is primarily due to the the CH_2 rocking mode. The displacements of the hydrogen atoms associated with this rocking mode are nearly perpendicular to the helix axis; this vibration has not, however, yet been located in the infrared absorption.

The Normal Vibrations of Poly(propylene-2-d) $[-CH_2-CD(CH)_3-]_n$

CH_2 Wagging and Twisting Modes.—As has been discussed before, the CH_2 wagging and twisting modes of $[-CH_2-CH(CH_3)-]_n$ are coupled with the CH bending modes. However, the CH_2 wagging and twisting modes of $[-CH_2-CD(CH_3)-]_n$ are almost free from the coupling with the CD bending modes, since the "intrinsic" CD bending frequencies are much lower than the 'intrinsic' CH_2 wagging and twisting frequencies. As Tables IV and V show, the parallel band of $[-CH_2-CD(CH_3)-]_n$ at 1342 cm^{-1} and the perpendicular band at 1334 cm^{-1} are associated almost exclusively with the CH_2 wagging mode. The parallel band at 1291 cm^{-1} and the perpendicular band at 1273 cm^{-1} are associated with the CH_2 twisting modes in accordance with the assignment made by Liang et al.[4]*6

The CH_2 wagging and twisting frequencies of propane are 1336 and 1278 cm^{-1} respectively.[11] These vibrations of propane are also free from much coupling with other modes. Therefore, the 'intrinsic' CH_2 wagging and twisting frequencies may be taken to be about 1335 cm^{-1} and 1280 cm^{-1} respectively.

CD Bending, CH_3 and CH_2 Rocking, and C–C Stretching Modes.—For $[-CH_2-CD(CH_3)-]_n$, eight parallel bands and seven perpendicular bands are observed[1] in the 1250～650 cm^{-1} region; all these bands arise from the hybridized vibrations of the CD bending, CH_3 rocking, CH_2 rocking, and C–C stretching modes. (No single band is due to a 'pure' mode.) All these modes have their intrinsic frequencies in the 1100～800 cm^{-1} region. For highly symmetric molecules, symmetry elements (such as twofold axes or planes of symmetry) impose restrictions upon the couplings among those vibrational modes, even though their 'intrinsic' frequencies lie in the same frequency region. However, the molecular chain of isotactic polypropylene does not have such symmetry elements, and all those vibrational modes of $[-CH_2-CD(CH_3)-]_n$ are subject to extensive hybridization.

The bands at 1060 (∥) and 1091 cm^{-1} (⊥) have been assigned to the C–D bending mode.[6] However, to judge from the normal coordinate analysis, these bands are not very much associated with the CD bending modes. Rather, the A vibration at 1060 cm^{-1} is due to the equatorial methyl rocking mode coupled with the CH_2 rocking mode, while, on the other hand, the E vibration at 1091 cm^{-1} is due to the equatorial methyl rocking mode coupled with the C-methyl stretching mode.*7

The parallel bands at 981, 969 and 790 cm^{-1} are the strongest peaks in the 1250～650 cm^{-1} region. The ν_{16}^{A} vibration is associated with the C-methyl stretching mode, the axial methyl rocking mode, and the axial CD bending

22) M. C. Tobin, *J. Opt. Soc. Am.*, **49**, 850 (1959).

*6 McDonald and Ward[6] also have assigned the bands at 1334 (⊥) and 1291 cm^{-1} (∥) to the CH_2 wagging and twisting modes respectively.

*7 Weak bands were observed at 1049 (∥) and 1016 cm^{-1} (⊥) and were assigned to CD bending modes.[6] These bands, however, are not identified in the spectra reported by Peraldo and Farina (Fig. 2b of Ref. 1).

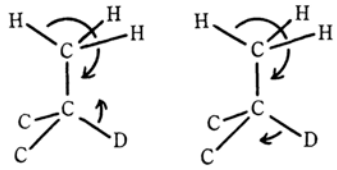

(a) (b)

Fig. 7. Schematic representations of the A vibrations of isotactic poly(propylene-2-d) at 790 cm^{-1} (a) and 1145 cm^{-1} (b).

mode. The ν_{17}^{A} vibration is associated with the methyl rocking mode perpendicular to the D–C–methyl plane as coupled with the axial C–C stretching mode.

The medium intensity band at 1210 cm^{-1} (∥) has been considered to be due to the coupling of the methyl rocking mode and the C–C stretching mode.[8] However, as Table IV shows, this band is due to the antisymmetric stretching mode of the axial and equatorial C–C bonds as coupled with the CD bending mode perpendicular to the D–C–methyl plane.

The strong parallel band at 790 cm^{-1} is due to the coupling of the CD bending mode and the CH_3 rocking mode (both in the D–C–methyl plane), as is schematically shown in Fig. 7a. On the other hand, the medium intensity band at 1145 cm^{-1} is primarily due to the other hybridization of the CD bending and methyl rocking modes, as shown in Fig. 7b. This vibration is, therefore, the counterpart of the A vibration at 790 cm^{-1}.

The CH_2 rocking mode (A species) of $(-CH_2-CD(CH_3)-)_n$ is strongly coupled with the CD bending mode (nearly perpendicular to the D–C–methyl plane). This band appears to be much stronger than the corresponding A vibration of $(-CH_2-CH(CH_3)-)_n$ calculated at 819 cm^{-1}. This is possibly due to the greater coupling of the CH_2 bending mode with the CD bending mode.

It is noteworthy that the perpendicular bands of $(-CH_2-CD(CH_3)-)_n$ are much weaker than the parallel bands observed in the 1250 ~650 cm^{-1} region although these E vibrations are also due to the hybridizations of the CD bending, CH_3 and CH_2 rocking, and C–C stretching modes, as are the A vibrations (Tables IV and V).

The Normal Vibrations of Poly(propylene-1, 1-d_2), $(-CD_2-CH(CH_3)-)_n$

CH Bending Modes.—As has been discussed before, the CH bending modes of $(-CH_2-CH(CH_3)-)_n$ are coupled with the CH_2 wagging and twisting modes. However, the CH bending modes of $(-CD_2-CH(CH_3)-)_n$ are almost free from couplings with the CD_2 wagging or twisting modes. As Tables VI and VII show, the parallel bands at 1327 and 1313 cm^{-1} and the perpendicular bands at 1325 and 1303 cm^{-1} are almost exclusively due to the CH bending modes. The CH bending displacements of the ν_{10}^{A} and ν_{11}^{E} vibrations are perpendicular to the H–C–methyl plane, whereas the CH bending displacements of the ν_{11}^{A} and ν_{10}^{E} vibrations are in the H–C–methyl plane.

The CH bending vibration of isobutane, which is observed at 1330 cm^{-1}, is not much coupled with other vibrational modes. Taking into account the CH bending frequencies of isobutane as well as of $(-CD_2-CH(CH_3)-)_n$, the 'intrinsic' CH bending frequency may be taken as ca. 1320 cm^{-1}.

CD_2 Rocking Modes.—The parallel band of $(-CD_2-CH(CH_3)-)_n$ at 691 cm^{-1} is primarily due to the CD_2 rocking mode, as Table VI shows. The intensity of this band is much stronger than the corresponding band (ν_{20}^{A}) of $(-CH_2-CH(CH_3)-)_n$. The perpendicular band at 716 cm^{-1} is due to the CD_2 rocking mode, coupled with the C–methyl stretching mode and the equatorial C–C stretching mode.

CD_2 Bending.—The perpendicular band at 1051 cm^{-1} corresponds to the calculated ν_{15}^{E} frequency of 1042 cm^{-1}, and this band is considered to be due to the CD_2 bending mode (Table VII). On the other hand, the strong parallel band at 1058 cm^{-1} appears to correspond to the ν_{15}^{A} vibration calculated at 1048 cm^{-1} or to the ν_{14}^{A} vibration calculated at 1082 cm^{-1}. The ν_{15}^{A} vibration is associated with the CD_2 bending mode, coupled with the equatorial methyl rocking mode. The ν_{14}^{A} vibration is associated with the hybridization of the axial methyl rocking mode and of the antisymmetric stretching mode of the C-methyl and C–C bonds.

CD_2 Wagging and Twisting Modes, CH_3 Rocking Modes, and C–C Stretching Modes.—The parallel band at 1134 cm^{-1} is due to the methyl rocking mode (in the H–C–methyl plane) coupled with the CD_2 twisting mode. The perpendicular band at 1110 cm^{-1} corresponds either to the ν_{14}^{E} vibration calculated at 1103 cm^{-1} or to the ν_{13}^{E} vibration calculated at 1128 cm^{-1}. The ν_{14}^{E} vibration is associated with the CD_2 wagging mode and the methyl rocking mode in the H–C–methyl plane.

The parallel band at 1184 cm^{-1} is due to the axial C–C stretching mode, coupled with the CD_2 wagging mode, whereas the perpendicular band at 1170 cm^{-1} is due to the equatorial C–C bond, coupled with the CD_2 bending mode. The nature of the infrared bands of poly(propylene-1, 1-d_2) in this region of the spectrum are too complicated for empirical analyses based on the isotope shifts.

The parallel bands at 894 and 868 cm^{-1} are due to the methyl rocking modes, coupled with the CD_2 wagging or twisting modes, as Table VI shows. The methyl rocking motion of the ν_{17}^A vibration (calculated at 900 cm^{-1}) is nearly perpendicular to the H–C-methyl plane, whereas the rocking motion of the ν_{18}^A vibration (calculated at 878 cm^{-1}) is nearly in the H–C-methyl plane. The parallel band at 1013 cm^{-1} arises from the antisymmetric stretching mode of the C-methyl and equatorial C–C bonds, coupled with the CD_2 wagging and methyl rocking mode.

The perpendicular band at 896 cm^{-1} is due to the methyl rocking mode (perpendicular to the H–C-methyl plane), coupled with the axial C–C stretching mode. The band due to the ν_{18}^E vibration is possibly overlapped by the strong parallel band at 868 cm^{-1}. The methyl rocking mode of the ν_{18}^E vibration is nearly in the H–C-methyl plane.

The weak parallel band at 764 cm^{-1} and the perpendicular band at 811 cm^{-1} are primarily due to the CD_2 twisting modes, as Table VI and VII show.

The Normal Vibrations of Poly(propylene-3, 3, 3-d_3), $[-CH_2-CH(CD_3)-]_n$

CH_2 Wagging and Twisting Modes and CH Bending Modes. — For isotactic $[-CH_2-CH\cdot(CD_3)-]_n$, four parallel bands and four perpendicular bands are observed in the 1400~1200 cm^{-1} region.[1] The absorption spectra in this region are very similar to the spectra of $[-CH_2-CH(CH_3)-]_n$. These bands arise from the coupling of the CH_2 wagging, CH bending, and CH_2 twisting modes, as Tables VIII and IX show*8. It may be seen that the A vibrations of $[-CH_2-CH(CD_3)-]_n$ at 1379, 1334, 1305 and 1239 cm^{-1} closely correspond to the A vibrations of $[-CH_2-CH(CH_3)-]_n$, except for a slight hybridization of the methyl symmetric deformation mode. Also the E vibrations of $[-CH_2-CH(CD_3)-]_n$ at 1361, 1333, 1293, and 1206 cm^{-1} correspond to the E vibrations of $[-CH_2-CH(CH_3)-]_n$ at 1360, 1330, 1296, and 1220 cm^{-1} respectively.

CD_3 Asymmetric Deformation Modes. — The strong parallel band at 1051 cm^{-1} corresponds to the ν_{14}^A and ν_{15}^A vibrations (calculated at 1049 and 1045 cm^{-1} respectively), and the strong perpendicular band at 1054 cm^{-1} corresponds to the ν_{15}^E and ν_{16}^E vibrations (calculated at 1044 and 1040 cm^{-1}, respectively). As Tables VIII and IX show, these bands are associated almost exclusively with the asymmetric deformation modes of the CD_3 group.

Liang et al. have assigned the bands at 1051 and 1054 cm^{-1} to the overlapped A and E components of all the asymmetric and symmetric deformation modes of the CD_3 group.[4] On the other hand, McDonald and Ward have assigned the strong bands at 1051 (∥) and 1145 cm^{-1} (⊥) to the symmetric and asymmetric deformation modes, respectively, of the CD_3 group.[6] As for the bands due to the symmetric modes, the present normal coordinate analysis favors the assignment made by Liang et al.

CD_3 Symmetric Deformation Mode.—The CD_3 symmetric deformation modes are strongly coupled with the C–C stretching modes. The weak parallel band at 1115 cm^{-1} appears to correspond to the ν_{13}^A vibration calculated at 1083 cm^{-1}. This vibration arises from a strong coupling between the CD_3 symmetric deformation mode and the C-methyl stretching mode. The perpendicular band at 1081 cm^{-1} corresponds either to the ν_{13}^E vibration calculated at 1079 cm^{-1} or to the ν_{14}^E vibration calculated at 1061 cm^{-1}. The ν_{13}^E vibration is associated with the axial and equatorial C–C stretching modes, coupled with the CD_3 symmetric deformation mode, whereas the ν_{14}^E vibration is primarily due to the CD_3 symmetric deformation mode, coupled with the asymmetric deformation mode. The parallel band at 989 cm^{-1} corresponds to the ν_{16}^A vibration and is due to the equatorial C–C stretching mode and the CD_3 symmetric deformation mode.

CD_3 Rocking Mode.—The parallel bands of $[-CH_2-CH(CD_3)-]_n$ at 791 and 703 cm^{-1} and the perpendicular bands at 759 and 743 cm^{-1} are associated almost exclusively with the CD_3 rocking modes, as Tables VIII and IX show.*9 The 'intrinsic' CD_3 rocking frequency appears to be much lower than the intrinsic frequencies of the CH_2 wagging and twisting modes or the C–C stretching mode. For the A vibration at 791 cm^{-1} and the E vibration at 759 cm^{-1}, the CD_3 rocking mode is nearly perpendicular to the H–C-methyl plane, whereas for the A vibration at 703 cm^{-1} and the E vibration at 743 cm^{-1} the CD_3 rocking mode is nearly parallel to the H–C-methyl plane.

CH_2 Rocking Mode and C–C Stretching Modes. —The parallel band at 807 cm^{-1} and the perpendicular band at 821 cm^{-1} are primarily due to the CH_2 rocking modes, coupled with the

*8 The bands at 1305 (∥) and 1293 (⊥) were assigned by Liang et al.[4] to the CH_2 twisting modes. The assignments by McDonald and Ward[6] were: 1379 (∥) and 1333 (⊥), CH_2 wag; 1293 (⊥), CH_2 twist; 1361 (⊥), 1305 (∥), 1239 (∥), and 1206 cm^{-1} (⊥), CH bend.

*9 The bands at 1081 (⊥), 909 (∥), and 791 cm^{-1} (∥) have been considered to be due in part to the CD_3 rocking modes.[6]

C-methyl or equatorial C–C stretching modes.*10 The parallel band at 909 cm^{-1} is due to the symmetric stretching mode of the C-methyl and equatorial C–C bonds (coupled with the equatorial CD_3 rocking mode and the CH_2 twisting mode). On the other hand, the strong perpendicular band at 1145 cm^{-1} is due to the C–methyl stretching mode and the CH bending mode.

The Liquid Spectra of Isotactic Polypropylene and Its Deuterated Derivatives

On the basis of the potential energy distributions as well as on that of the normal modes calculated for the crystalline spectra, one may also assign the bands observed in the liquid spectra of isotactic polypropylene and its deuterated derivatives.

Localized Modes.—The effect of melting upon the infrared spectra of isotactic polypropylene[23,24] and its deuterated derivatives[1] have been studied, and several absorption bands have been found to persist upon melting. For example, strong bands are observed at 1380 cm^{-1} and 1460 cm^{-1} for $[-CH_2-CH(CH_3)-]_n$, $[-CH_2-CD(CH_3)-]_n$, and $[-CD_2-CH(CH_3)-]_n$, but not for $[-CH_2-CH(CD_3)-]_n$. These peaks are assigned to the symmetric and asymmetric deformation modes, respectively, of the methyl group. Similarly, for $[-CH_2-CH(CD_3)-]_n$ in the liquid state, a strong band is observed at 1052 cm^{-1}. This band corresponds to the strong bands at 1054 ($\parallel$) and 1051 cm^{-1} ($\perp$) in the crystalline state and is assigned to the asymmetric deformation modes of the CD_3 group in the liquid state.

The strong band at 1446 cm^{-1} is observed for $[-CH_2-CH(CD_3)-]_n$ and is assigned to the CH_2 bending mode. For $[-CH_2-CH(CH_3)-]_n$ and $[-CH_2-CD(CH_3)-]_n$ in the liquid state, the band due to the CH_2 bending mode is overlapped by the strong band arising from the asymmetric methyl deformation modes. For $[-CD_2-CH(CH_3)-]_n$, a medium intensity band is observed at 1057 cm^{-1}. This band appears to correspond to the ν_{15}^{A} (1058 cm^{-1}) and ν_{15}^{E} vibration (1051 cm^{-1}) and is assigned to the CD_2 bending mode.

The frequencies of the symmetric and asymmetric deformation vibrations of the CH_3 group or the bending vibrations of the CH_2 group do not shift essentially upon melting. As Tables II–IX show, the potential energy of these vibrations is concentrated in one vibrational mode, while the atomic displacements are localized in the methyl or the methylene groups. Therefore, even though the main chain of isotactic polypropylene carries out internal-rotation rearrangements above the melting point, these localized vibrations of the methyl or the methylene groups are not very much influenced by the thermal motions of the backbone chain. The bands arising from localized vibrations in the liquid state may be as strong and sharp as the corresponding bands in the crystalline state.

CH_2 Wagging and Twisting Modes.—On the basis of these considerations, it would be anticipated that the bands due to 'localized' vibrations in the liquid state will be stronger and more well-defined as the localization becomes higher. In fact, for $[-CH_2-CD(CH_3)-]_n$, a strong band is observed at 1333 cm^{-1}; this band is assigned to the CH_2 wagging mode in the liquid state. As has been discussed before, the CH_2 wagging vibration of this molecule is free from coupling with other modes, and its vibrational displacements are much localized in the $C-CH_2-C$ group. The frequency of this band agrees closely with the 'intrinsic' CH_2 wagging frequency taken at 1335 cm^{-1}. In the crystalline state, the CH_2 wagging frequencies ($\nu_{11}^{A}=1342$ cm^{-1} and $\nu_{11}^{E}=1334$ cm^{-1}) are split by 8 cm^{-1}.

The liquid band of $[-CH_2-CD(CH_3)-]_n$ at 1282 cm^{-1} corresponds to the 'intrinsic' CH_2 twisting frequency of 1280 cm^{-1} and is assigned to the CH_2 twisting mode in the liquid state. As has been discussed before, the twisting mode of this molecule is also free from much coupling with other vibrational modes, and the vibrational displacements are greatly localized in the $C-CH_2-C$ group. In the crystalline state, the twisting frequencies are split into the A component at 1291 cm^{-1} and the E component at 1273 cm^{-1}.

CH Bending Modes.—For $[-CD_2-CH(CH_3)-]_n$, a strong band is observed at 1318 cm^{-1} in the liquid state. This band corresponds to the 'intrinsic' CH bending frequency of 1320 cm^{-1}. The CH bending vibrations of this molecule are not much coupled with other vibrational modes.

For $[-CH_2-CH(CD_3)-]_n$ in the liquid state, four bands are observed[1] at 1358, 1326 (shoulder), 1293, and 1235 cm^{-1}. These peaks arise from the CH_2 wagging and twisting modes and the CH bending modes in the liquid state. These frequencies, however, are shifted slightly but distinctly from the 'intrinsic' frequencies of the CH_2 wagging, twisting and CH bending modes, indicating vibrational couplings among these modes, even in the liquid state. Vibrational couplings among these

*10 The parallel band at 710 cm^{-1} was assigned to the CH_2 rocking mode by McDonald and Ward.[6]

23) G. Natta, *J. Polymer Sci.*, 16, 143 (1955).

24) K. Abe and K. Yanagisawa, ibid., 36, 536 (1959).

modes should depend upon the internal-rotation conformations about the axial and equatorial C–C bonds. Therefore, theoretical analyses of these couplings will be useful for conformation studies of isotactic polypropylene chains in the liquid state.

CD_3 Rocking Modes. — For $[-CH_2-CH\cdot(CD_3)-]_n$ in the liquid state, two medium-intensity bands are observed at 790 and 709 cm^{-1}. The band at 790 cm^{-1} corresponds to the ν_{19}^A (791 cm^{-1}) and ν_{19}^E vibrations (759 cm^{-1}) of the crystalline state, vibrations which are associated with the CD_3 rocking mode perpendicular to the H–C-methyl plane. On the other hand, the liquid band at 709 cm^{-1} corresponds to the ν_{20}^A (703 cm^{-1}) and ν_{20}^E vibrations (743 cm^{-1}), which are associated with the CD_3 rocking mode in the H–C-methyl plane. As Tables VIII and IX show, these vibrations of the crystalline state are associated exclusively with the CD_3 rocking modes, and the vibrational displacements are localized, at least in the $CD_3-CH\langle^{C}_{C}$ group. These CD_3 rocking modes involve the vibrational displacement of the main-chain carbon atoms and, in fact, the A and E frequencies of the ν_{19} or ν_{20} vibrations are split by 30~40 cm^{-1}. These splittings are reduced upon melting when the main chain conformations are not rigid. On the other hand, the internal rotation conformation of the $CD_3-CH\langle^{C}_{C}$ group does not change upon the rearrangement of the CD_3 group from one staggered form to another. Therefore, the CD_3 rocking modes are not influenced by the internal rotation of the CD_3 group, and well-defined bands due to the CD_3 rocking modes may well be expected, even in the liquid state. Accordingly, the liquid band at 790 cm^{-1} is assigned to the CD_3 rocking mode perpendicular to the H–C-methyl plane, whereas the band at 709 cm^{-1} is assigned to the CD_3 rocking mode in the H–C-methyl plane.

The CD_3 rocking frequencies of perdeuterated ethane, C_2D_6, are observed at 970 cm^{-1} (E_g) and 594 cm^{-1} (E_u). Since the splitting of these rocking frequencies arises from the trans- and gauche-coupling potential term,[9,11] the 'intrinsic' CD_3 rocking frequency may be taken to have an average value of about 780 cm^{-1} [~(970+594)/2]. The CD_3 rocking vibration of $[-CH_2-CH(CD_3)-]_n$ at 790 cm^{-1} corresponds to the intrinsic frequency derived from deuteroethane.

CH_3 Rocking and C–C Stretching Modes.— For $[-CH_2-CH(CH_3)-]_n$ two strong bands are observed at 1151 cm^{-1} and 971 cm^{-1} in the liquid state. These liquid bands are possibly associated with 'localized' vibrational modes of the $CH_3-CH\langle^{C}_{C}$ group modes, which are not influenced by the internal rotation rearrangements, at least of the CH_3 group.

The intrinsic CH_3 rocking frequency may be estimated at about 1000 cm^{-1} [~(1190+821)/2] from the CH_3 rocking frequencies (E_g: 1190 cm^{-1} and E_u: 821 cm^{-1}). The liquid band of $[-CH_2-CH(CH_3)-]_n$ at 971 cm^{-1} corresponds to this intrinsic frequency and is considered to be associated primarily with the CH_3 rocking modes in the liquid state. On the other hand, the contributions of the C–C stretching modes are possibly greater for the liquid band at 1151 cm^{-1} than that of the methyl rocking mode. Since the degenerate C–C stretching vibration of isobutane,[11] $CH_3-CH\langle^{CH_3}_{CH_3}$, is observed at 1166 cm^{-1}, the liquid band of polypropylene at 1151 cm^{-1} is possibly associated with the asymmetric stretching mode, coupled with the methyl rocking mode of the $CH_3-CH\langle^{C}_{C}$ group. Naturally, these tentative assignments should be examined further by means of theoretical treatment of the liquid spectra. Nevertheless, these considerations are supported by the observation of a corresponding strong band at 1140 cm^{-1} in the liquid spectra of $[-CH_2-CH(CD_3)-]_n$, a band which may not be ascribed to the methyl rocking mode. More extensive analyses of the liquid spectra of isotactic polypropylene and deuterated derivatives will be important for conformation studies of the isotactic polymeric chain, and, accordingly, theoretical developments in the treatment of the liquid spectra of flexible polymeric chains are highly desirable.

Summary

The infrared active normal vibrations of isotactic polypropylene and its deuterated derivatives in the crystalline state have been treated by the general method derived previously.[8] The modified Urey-Bradley force field has been used; the trans- and gauche-coupling potential terms for the H–C–C angles and the angle-interaction terms for the methylene group have been added to the Urey-Bradley force field. A total of 16 potential constants have been adjusted by the method of least squares, and a total of about 100 infrared-active frequencies have been calculated with the r. m. s. frequency deviation as small as 1.1%. The potential energy distributions have been calculated, together with the normal modes, and the nature of the inferred bands observed in the 1500~650 cm^{-1} region

have been elucidated. Vibrational assignments for the well-defined liquid bands of isotactic polypropylene and its deuterated derivatives have also been made.

The authors wish to thank Professor Takehiko Shimanouchi of the University of Tokyo for his encouragement and his stimulating discussions and Dr. Kunio Fukushima of Osaka University and Dr. Takaharu Ohnishi and Dr. Hiroaki Takahashi of the University of Tokyo for their helpful discussions.

Institute for Protein Research
Osaka University
Kita-ku, Osaka